

Extension of the Dip-test Repertoire - Efficient and Differentiable p-value Calculation for Clustering

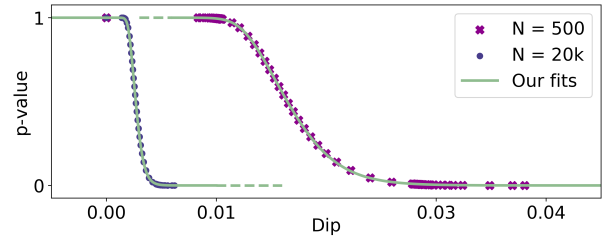
Lena G. M. Bauer^{*,†,‡}Collin Leiber^{*,§}Christian Böhm[†]Claudia Plant[†]

Abstract

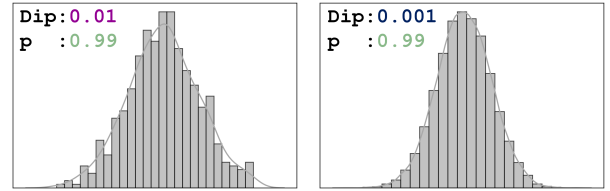
Over the last decade, the Dip-test of unimodality has gained increasing interest in the data mining community as it is a parameter-free statistical test that reliably rates the modality in one-dimensional samples. It returns a so called Dip-value and a corresponding probability for the sample's unimodality (Dip-p-value). These two values share a sigmoidal relationship. However, the specific transformation is dependent on the sample size. Many Dip-based clustering algorithms use bootstrapped look-up tables translating Dip- to Dip-p-values for a certain limited amount of sample sizes. We propose a specifically designed sigmoid function as a substitute for these state-of-the-art look-up tables. This accelerates computation and provides an approximation of the Dip- to Dip-p-value transformation for every single sample size. Further, it is differentiable and can therefore easily be integrated in learning schemes using gradient descent. We showcase this by exploiting our function in a novel subspace clustering algorithm called Dip'n'Sub. We highlight in extensive experiments the various benefits of our proposal.

1 Introduction

One of the major goals in data mining is to automatically find meaningful patterns and structures in data. This is ideally done fast and with as few hyperparameters as possible. Here, the definition of statistical modes plays a decisive role in many approaches. Clustering methods like MeanShift [6] or Quickshift [28] try to find modes with the help of a predefined influence area and assign objects to these modes. Other procedures focus on evaluating whether a data set has a single or multiple modes. Examples are Hartigan's Dip-test [11], the Silverman test [27], the Folding Test [26] or the recently presented UU-test [5]. In clustering the assumption for these methods is that multiple modes indicate multiple clusters, while unimodality is a sign for a single clus-



(a) Bootstrapped (Dip, p) -pairs and our fitted functions.



(b) $X \sim \mathcal{N}(0, 1)$, $N = 500$. (c) $X \sim \mathcal{N}(0, 1)$, $N = 20k$.

Figure 1: (a) Bootstrapped (Dip, p) -pairs for sample sizes $N = 500$ (purple) and $N = 20k$ (blue) and our fitted functions (green). The transformation function from Dip- to Dip-p-value strongly depends on the sample size. (b) and (c) Histograms of samples from a $\mathcal{N}(0, 1)$ normal distribution with sample size $N = 500$ and $N = 20k$. When applying the Dip-test on the two samples, their Dip-values differ with a factor of 10. The respective Dip-p-values are, however, 0.99 in both cases.

ter. The tests are basically parameter-free, which makes them particularly interesting for the data mining community. The most commonly used unimodality test in the clustering domain is probably the Dip-test. The input for the Dip-test is a one-dimensional sample and the test outputs a Dip-value $Dip \in (0, 0.25]$ that can be converted to a p-value, which we will term Dip-p-value throughout this work. The latter represents a probability for the sample to be unimodal and it is high for Dip-values close to zero and low for Dip-values close to its maximum of 0.25. Its benefits have already been exploited by several data mining techniques.

DipMeans [13], projected DipMeans [4], SkinnyDip [18], M-Dip [7], NrDipMeans [20] and DipDECK [16], for example, are all algorithms that use the Dip-test to

^{*}Authors contributed equally.

[†]Faculty of Computer Science, ds:UniVie, University of Vienna, Vienna, Austria. {lena.bauer, christian.boehm, claudia.plant}@univie.ac.at

[‡]UniVie Doctoral School Computer Science.

[§]LMU Munich & MCML, Munich, Germany. leiber@dbs.ifl.lmu.de

estimate the number of clusters. Other algorithms like DipTransformation [25], DipExt [24] or the DipEncoder [15] utilise the Dip-test to create cluster-friendly lower-dimensional spaces. When executing these algorithms, a precise and efficient determination of the Dip- and Dip-p-value is of high relevance. In general, the Dip-value translates sigmoidal to the Dip-p-value. Figure 1a clearly shows the pattern. Importantly, we can observe that the specific curvatures and positions of the sigmoidal functions are heavily dependent on the number of samples N . Figures 1b and 1c show that the Dip-p-values p of a normal distribution $\mathcal{N}(0, 1)$ with $N = 500$ and $N = 20k$ are both 0.99. This is in accordance to the expectation of the normal distribution to be unimodal irrespective of the sample size. The Dip-values Dip , however, differ by a factor of 10. Thus, considering the Dip-p-value is a far more robust choice when optimising for uni- or multimodality.

To the best of our knowledge, however, there exists no elegant method for the translation from Dip- to Dip-p-value. The state-of-the-art procedure is to utilise a look-up table with a limited amount of pairs of Dip- and Dip-p-values and use \sqrt{N} -interpolation to provide the missing pairs in between table values. While this approach has been used in multiple procedures (e.g., [4, 13, 16, 18, 20]), it shows drawbacks in several aspects. First, it is not differentiable and therefore harder to integrate into strategies such as stochastic gradient descent (SGD) and second, it is limited to the maximum bootstrapped sample size in the table. To resolve these shortcomings we propose a differentiable transformation function which - provided with a Dip-value and the number of samples - automatically calculates the corresponding Dip-p-value (see green lines in Fig. 1a). We showcase the practical value of our proposal for data mining research by developing a subspace clustering algorithm, that exploits the differentiability of our transformation function to identify a common subspace for all clusters in the data set. This helps to analyse relationships between clusters [10, 19] and distinguishes us from ‘classical’ subspace clustering algorithms (e.g., ORCLUS [1] or 4C [2]) which find a separate subspace for each cluster. Our idea uses the gradient of the Dip-p-value to identify projection axes where all clusters show a high degree of multimodality by performing SGD. This approach makes it particularly apt to rely on the Dip-p-value instead of the Dip-value as different cluster sizes bias the latter. Further, we present TailoredDip, an extended version of the one-dimensional clustering procedure UniDip [18], to cluster the data on those axes.

Our contributions can be summarised as follows:

- We provide a fully automatic translation from Dip- to Dip-p-value via an analytical function (Sec. 3.2)

- The translation is available for any data size N and provides reliable Dip-p-values irrespective of the underlying distribution (Sec. 4.1)
- Analyses show that our novel calculation is faster than previously used methods, in particular bootstrapping (Sec.4.2)
- We showcase how the differentiability of our function is useful for practical data mining applications by introducing our subspace clustering algorithm Dip’n’sub (Sec. 3.3 and 4.3)

2 Related Work

2.1 The Dip-test The Dip-test is a statistical test for modality in a one-dimensional sample developed by Hartigan and Hartigan [11]. The test returns a so-called Dip-value Dip that specifies the distance between the Empirical Cumulative Distribution Function (ECDF) of the sample to an unimodal piece-wise linear function, i.e., a function that is convex up to the beginning of the steepest slope and concave thereafter. In this context, the area of steepest slope is often called *modal interval*. By definition $Dip \in (0, 0.25]$, where a Dip close to 0 indicates a unimodal distribution and a $Dip \gg 0$ indicates a multimodal distribution. The exact value not only depends on the specific distribution but also on the sample size (see Fig. 1b and 1c). For this reason, Dip-values are often not used directly, but the associated Dip-p-values. Here, the null hypothesis \mathcal{H}_0 states that the sample set is unimodal and the alternative hypothesis \mathcal{H}_1 is that there are at least two modes present in the data. The test does not make any assumptions about the data generating distribution. For any distribution with a single mode, whether it is Gaussian, Laplacian or t-distributed the test will not reject \mathcal{H}_0 . The Dip-test can be calculated efficiently in $O(N)$ [11] on a sorted input of size N . Furthermore, [14] showed that the Dip-value is differentiable with respect to a projection axis. This enables the use of SGD. Due to these several benefits, the Dip-test has successfully been integrated in several data mining applications over the last decade.

2.2 Bootstrapping The Dip-test can convert a Dip-value to a p -value representing an evidence measure for the credibility of the null hypothesis. The original work by Hartigan and Hartigan [11] provides a table with bootstrapped Dip-values and corresponding Dip-p-values for samples of different sizes N . The table lists the relationships for 13 different sample sizes ranging between 4 and 200 with 9 (Dip, p)-pairs each. These were calculated by drawing N random samples from a uniform distribution several times. The Dip-test was

then performed on each of these sample sets. The percentage of sets with a Dip-value smaller than the input Dip-value thus gives the respective Dip-p-value. The idea is that the uniform distribution represents a borderline case between unimodal and multimodal distributions [11]. In previous publications authors used bootstrapping to enlarge Hartigan and Hartigan’s table to a total of 21 sample sizes up to 72,000 data points with 26 (Dip, p)-pairs for each sample size. They use interpolation of \sqrt{N} to get intermediate Dip-p-values. To the best of our knowledge this approach is the state-of-the-art when transforming Dip- to Dip-p-value.

2.3 Dip-test Related Data Mining Most clustering methods utilising the Dip-test are dedicated to the estimation of the number of clusters in a data set. Here, an essential component is the transformation of the data into a one-dimensional space where the Dip-test can be applied. One of the first approaches is DipMeans [13], which uses the Dip-test to determine if the distances between data points within a cluster are distributed unimodally. For projected DipMeans [4] the input for the Dip-test are the data points itself, after they have been projected onto projection axes. Another transformation is applied by M-Dip [7]. Here, the Dip-test is executed on the path of closely located points between two clusters. NrDipMeans [20] estimates the number of clusters in a non-redundant clustering setting by employing a Dip-based splitting strategy. The first clustering and k -estimation technique using the Dip-test in a deep learning context is DipDECK [16], which uses the test to decide whether clusters should be merged or not. SkinnyDip [18] determines clusters in highly noisy data sets by running its subroutine UniDip on each feature of each cluster. UniDip recursively executes the Dip-test to identify modal intervals (see Sec. 2.1) in the one-dimensional data set until all intervals themselves and the areas left and right (until the next interval) are considered unimodal. Finally, each modal interval is considered a cluster and all objects that do not fall within such an area are classified as noise. The idea of SkinnyDip is later used to cluster streaming data with StrDip [17]. All of the mentioned procedures need to decide whether samples are distributed unimodally or not and, therefore, use the same bootstrapped look-up table to convert Dip-values into probabilities.

An example for a Dip-based pre-processing algorithm is DipTransformation [25]. It scales and transforms a data set, such that the resulting feature space is suitable for k-means. In DipExt [24] this idea is extended by making use of the differentiability of the Dip-value with respect to the projection axis. Structure-rich features are extracted from the data by searching for

suitable projection axes with SGD. The DipEncoder [15] uses the gradient of the Dip-value to train an autoencoder in such a way that each combination of clusters projected onto their specific projection axis is highly multimodal in the embedding.

2.4 Common Subspace Clustering Traditional subspace clustering algorithms like 4C [2] or ORCLUS [1] define an individual subspace for each cluster. In this setting, however, the inter-cluster relationships are difficult to analyse [10]. We would therefore like to identify a common subspace for all clusters. A simple possibility to find such subspaces are dimensionality reduction techniques such as Principal Component Analysis (PCA) [21], Independent Component Analysis (ICA) [12], Linear Discriminant Analysis (LDA) [9] or the already mentioned DipExt [24] algorithm. Since in these cases possible cluster assignments do not influence the final subspace, special common subspace clustering algorithms like LDA-k-means [8], FOSSCLU [10] and SubKmeans [19] have been developed. LDA-k-means and SubKmeans utilise LDA or an eigenvalue decomposition, respectively, in combination with the k-means objective to determine the subspaces. FOSSCLU combines the EM algorithm with rigid transformations.

3 Methods

In this section, we design a special sigmoid function converting Dip- to Dip-p-values. This function’s differentiability is then exploited by our subspace clustering algorithm Dip’n’Sub.

3.1 Table Extension To increase the granularity level of the look-up table previously used in literature, we also use bootstrapping as proposed by [11]. We sample from uniform distributions with 100,000 repetitions to obtain a Dip-p-value table containing 307 (Dip, p)-pairs for 63 sample sizes up to a sample size of 150,000 data points. This look-up table provides a good basis, but it does not cover all values of sample sizes N . Therefore, we fit a logistic function $p(\cdot)$ to provide a differentiable solution for this issue. Fig. 3 visually captures Sec. 3.1 and Sec. 3.2.

3.2 Function Fit A good fitting function provides high flexibility to fit the different sigmoidal relationships between Dip- and Dip-p-value for all sample sizes N while using the smallest possible number of parameters. Due to the sigmoidal behaviour it is reasonable to approximate it with a generalised logistic function [22].

$$l(Dip) = d + \frac{a - d}{(c + h \cdot e^{-b \cdot Dip})^{1/g}}$$

The parameters a and d represent the upper and lower asymptote, respectively, and need to be fixed as $a = 1$ and $d = 0$ in our application as we model probability values. In addition, $c = 1$ must hold for the function to actually be constrained by 1. Further, often $h = g$ applies (see e.g. [3]). To obtain a negative slope, b needs to be positive. Another requirement is that $g > 0$ holds. This essentially leaves the parameters $h = g$ and b , which mainly determine the curvatures. However, we also need to adjust the scale for the x-axis since the Dip-value is limited within $(0, 0.25]$. Therefore, we have to include a shift parameter in the exponential function. Finally, we want to account for highly different curvatures at the two asymptotes and therefore include a weighting, which is partly inspired by the work of [23]. Our final fitting function reads as follows:

$$p(x, \theta_N) = 1 - \left[w_N \cdot (1 + h_N \cdot e^{-q_N \cdot x + s_N})^{1/h_N} + (1 - w_N) \cdot (1 + k_N \cdot e^{-r_N \cdot x + u_N})^{1/k_N} \right]^{-1},$$

with the independent variable x and where $\theta_N = (w_N, h_N, k_N, q_N, r_N, s_N, u_N)$ is the set of parameters. We then optimise θ_N with respect to the mean squared error between the fitting function and our enlarged table values for each sample size N separately. We find that most of the parameters are approximately constant across sample sizes N . Thus, we set them to the mean value across all N to reduce the number of parameters. Hence, it is sufficient to set w_N, h_N, k_N, s_N and u_N as constants and further set $q_N = r_N = b_N$ as the one remaining parameter depending on the sample size N . The resulting optimal values for b_N are shown in Fig. 2 (teal stars). As they visually resemble a square root function of N , we model the parameter b_N as the following function of N :

$$b(N) = b_1 \cdot \sqrt{N} + b_2.$$

Note, that b_1 and b_2 are parameters independent of N . The final optimisation is to find b_1 and b_2 such that

$$\mathcal{E}(b_1, b_2) = \frac{1}{|\mathcal{S}|L} \sum_{N \in \mathcal{S}} \sum_{i=1}^L (p_{Dip_i, N} - \hat{p}(Dip_i, \hat{b}(N)))^2$$

is minimal. Here, \mathcal{S} is the set of all sample sizes N , where $|\mathcal{S}| = 63$ in the case of our enlarged table, and L is the number of (Dip, p) -pairs in the extended table, here $L = 307$. The optimal function within our optimisation scheme with respect to the mean squared error and with

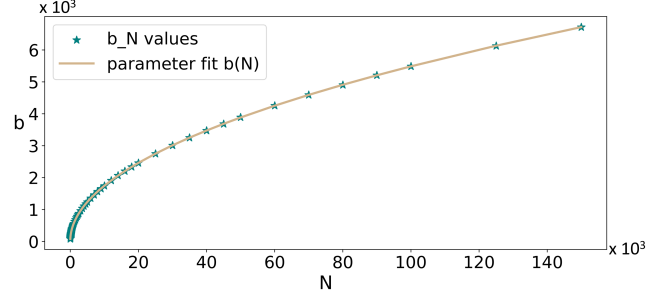


Figure 2: Our fitted function for the parameter b_N .

our bootstrapped table as data to be fitted is given by

$$\hat{p}(x, \hat{b}(N)) = 1 - \left[0.6 \cdot (1 + 1.6 \cdot e^{-\hat{b}(N) \cdot x + 6.5})^{1/1.6} + 0.4 \cdot (1 + 0.2 \cdot e^{-\hat{b}(N) \cdot x + 6.5})^{1/0.2} \right]^{-1},$$

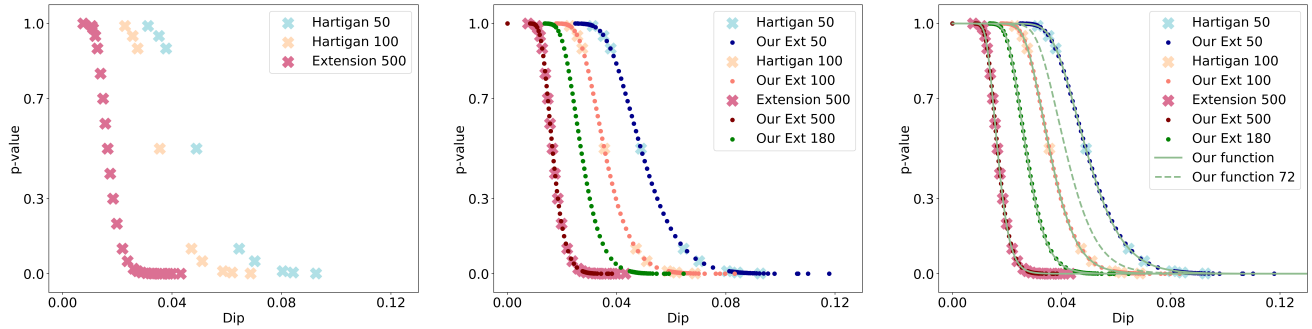
and

$$\hat{b}(N) = 17.30784 \cdot \sqrt{N} + 12.04918$$

where values for $\hat{b}_1 = 17.30784$, $\hat{b}_2 = 12.04918$ are rounded to five decimal places and correspond to the optimal estimators for b_1 and b_2 . The concatenated function $\hat{p}(x, \hat{b}(N))$ is smooth and well-defined for all $N \in \mathbb{N}^+$ and all $x \in (0, 0.25]$.

Derivation: One of the benefits of our proposal is, that the fitted function is differentiable. This property is exploited in our later discussed subspace clustering algorithm. The Dip-test can only be applied to a one-dimensional sample, which is why we always consider a projection axis ρ for d -dimensional data sets X . Further, the data has to be sorted. Thus, the Dip-value is returned for the sorted and projected data \bar{X}_ρ . From [14] we know that we can calculate the gradient vector of the Dip-value on \bar{X}_ρ with respect to the projection axis ρ . We will term this gradient $\nabla_\rho(Dip(\bar{X}_\rho))$. Details about the calculation of this gradient can be found in [14, 15, 18, 24]. By using our differentiable sigmoid function to calculate the Dip-p-value of the Dip , the Dip-p-value is also continuously differentiable as a concatenation of differentiable functions. The gradient is the following, where we define $D := Dip(\bar{X}_\rho)$ and $b := \hat{b}(N)$ for easier readability:

$$\nabla_\rho(\hat{p}(D, b)) = (-b \nabla_\rho(D)) e^{-bD + 6.5} \cdot \left[0.6(1 + 1.6e^{-bD + 6.5})^{\frac{1}{1.6}} + 0.4(1 + 0.2e^{-bD + 6.5})^{\frac{1}{0.2}} \right]^{-2} \cdot \left[0.6(1 + 1.6e^{-bD + 6.5})^{\frac{-0.6}{1.6}} + 0.4(1 + 0.2e^{-bD + 6.5})^{\frac{0.8}{0.2}} \right]$$



(a) Examples of (Dip, p) -pairs from the original table [11] and an example of an extensions for $N = 500$ (b) We bootstrap with larger granularity for N as well as (Dip, p) -pairs. (c) Our differentiable fitted function closes the remaining granularity gaps for all N and all (Dip, p) -pairs.

Figure 3: (a) Hartigan and Hartigan’s original bootstrapped table only provides pairs of Dip- and Dip-p-values for 13 different sample sizes. This table has been extended to values of $N \geq 500$. (b) We enlarge the table for even more values of N as well as a larger granularity regarding (Dip, p) -pairs (for better visualisation, we down-sampled our table to every third point). (c) We close the remaining gaps by providing our fitted function, such as for $N = 72$, for which we do not have bootstrapped values.

3.3 Dip’n’Sub We aim to show with a proof-of-concept that our differentiable Dip-p-value function has great value for the data mining community. Therefore, we present the subspace clustering algorithm Dip’n’Sub which is solely based on the Dip-test. It is able to automatically define a lower-dimensional subspace and also to derive the number of clusters. For this, only a significance threshold is necessary, which indicates whether a distribution is unimodal. We first propose TailoredDip, a new extension of UniDip [18].

A problem with UniDip is that the tails of distributions are very generously identified as outliers. TailoredDip is able to better capture those tails. We achieve this by checking the spaces between the clusters for additional structures after the regular UniDip algorithm has terminated. Therefore, we mirror the respective area between two clusters and calculate the Dip-p-value. If this indicates multimodal structures, we identify appropriate modes and assign those points to the best fitting neighbouring cluster. Further, if outlier detection is not desired we use the following strategy to assign them either to the left or the right cluster: Instead of simply defining the mid point between neighbouring clusters as a decision boundary, we choose the point that corresponds to the intersection of the ECDF and the line between the right limit of the left cluster and the left limit of the right cluster. This handles different tails more accurately. Details about TailoredDip as well as a pseudocode are given in the supplement (Sec. 1).

Now that we can find clusters in one-dimensional samples, let us consider the multidimensional case. Here, we use the fact that SGD can be used to find a pro-

jection axis on which a data set shows a minimum Dip-p-value. A naive approach would be to recursively select each cluster and, using the points of that cluster, find the projection axis on which those samples exhibit the greatest multimodality. The problem here is twofold. First, there is almost always some degree of multimodality in a set of objects, which means that one will identify a very high number of clusters. Second, the individual clusters are difficult to compare with each other, since each cluster forms its own subspace. Therefore, we want to successively identify those features in which as many objects as possible are contained in highly multimodal clusters. Thus, we recursively search for projection axes ρ that minimise the following term:

$$(3.1) \quad \frac{1}{N} \sum_{i=1}^k |C_i| \hat{p}(\text{Dip}(\overline{C}_i^\rho), \hat{b}(|C_i|)),$$

where C_i are the samples in cluster i and \overline{C}_i^ρ are the same samples projected to ρ and sorted afterwards, i.e. $\overline{C}_i^\rho = \text{sort}\{\rho^T c | c \in C_i\}$. To find these axes, we are inspired by [24]. We start with the q features that show the lowest sum of Dip-p-values weighted by their cluster sizes and use them as starting points for SGD with momentum. Further, we start at the first q components of a PCA. [24] has shown that $q = \log(d)$ is sufficient, where d is the original number of features. Using these $2q$ starting axes, we iteratively calculate the gradient with respect to all clusters. Here, we exploit that our fitted function enables us to directly calculate the gradient of Eq. 3.1. Having identified the best projection axis, we check whether more than

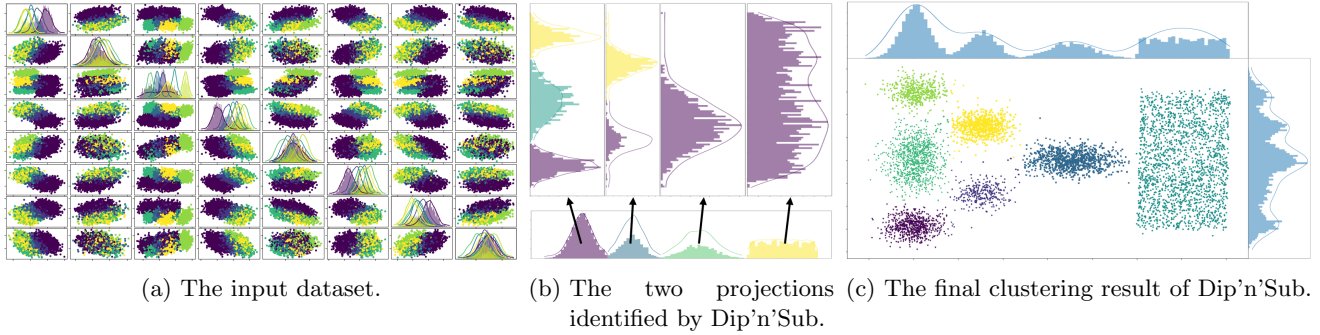


Figure 4: **(a)** Scatter matrix plot of an 8-dimensional synthetic data set (colours correspond to ground-truth labels). **(b)** The horizontal histogram below illustrates the first projection identified by Dip'n'Sub. The data is highly multimodal and therefore divided into 4 clusters. Dip'n'Sub now uses these cluster assignments to identify a second projection in which all clusters are as multimodal as possible. The second projection is shown vertically in the upper histograms, with respect to each existing cluster individually. It is easy to see that the first two clusters (purple and blue) are subdivided into 3 and 2 clusters, respectively. Thereafter, no multimodal third projection can be found. **(c)** The final clustering result of Dip'n'Sub reveals a clear separation of the clusters.

$T\%$ of the objects are contained in clusters considered multimodal on this axis, where T has to be set by the user. If this is the case, we apply TailoredDip to this axis. Each cluster is considered individually and divided into several sub-clusters. The clusters thereby form hypercubes in the final feature space. Our method Dip'n'Sub is presented in Algorithm 1 and an example of the subspace identification process is shown in Fig. 4.

4 Experiments and Results

We will show the several benefits of our proposal in three main experimental sections. First, we show, that our calculated Dip-p-values are as reliable as the ones with the look-up table. Then we present runtime experiments that prove our method to be efficient, not only in ‘laboratory conditions’, but also in practice when integrated in existing methods using Dip-p-values. Finally, we evaluate our subspace clustering algorithm Dip'n'Sub to showcase the integration of the gradient of the Dip-p-value in a practical data mining application.

Our supplement, codes, enlarged (Dip, p) -pairs table and the used data sets are available at: <https://dx.doi.org/10.6084/m9.figshare.21916752>.

4.1 Reliable Computation One important advantage of our fitted function is, that it provides Dip-p-values for all sample sizes N . Table 1 shows that our ‘function’ method is consistent with the look-up ‘table’ and ‘bootstrap’ methods as we produce basically the same Dip-p-values, not only for different unimodal distributions ($\mathcal{N}(4,1)$ = normal distribution with centre 4 and variance 1; $\mathcal{T}_{nc}(4,2,0,1)$ = non central student’s t-distribution with 4 degrees of freedom, non-centrality

parameter 2, centre 0 and scaling 1; $\mathcal{L}(0,2)$ = Laplace distribution with centre 0 and scaling 2), but also for multimodal distributions, which we create by combining samples of the same unimodal distribution, but with a different centre. In the supplement (Sec. 2.3) we show tables with a total of 23 distributions, where we observe the same behaviour.

Comparing to the enlarged bootstrapped table described in Sec. 3.1 our function performs better than the ‘table’ method, with the quality of both methods being measured in mean squared error (MSE). In this case, bootstrapping can be seen as some kind of ground truth, however it is not practical as runtime is a major issue, especially for large N . We will see this in more detail in the next section. Regarding the ‘table’ method, errors for sample sizes greater than 72,000 had to be ignored for the calculation of this MSE, because it cannot provide any Dip-p-values in that case. While we achieve an MSE of $3.43 \cdot 10^{-6}$ for all N , the ‘table’ results in an MSE of $7.92 \cdot 10^{-6}$. To check how well our function generalises with respect to N , we calculate the MSE for a set of N chosen as the mean values between each two N of our enlarged table. Those 62 values were not used for our function fit. The result is an MSE of $3.14 \cdot 10^{-6}$ for ‘function’ and $8.12 \cdot 10^{-6}$ for ‘table’. Hence, we outperform the ‘table’ method in both cases.

4.2 Computing Time In the first experiment, we sum up the runtimes of all the Dip-p-value calculations for the 23 distribution cases shown in the supplement (Table 1 is a selection of six of them). These are shown in Fig. 5. Note, that the y-scale is logarithmic. Note also the missing value for $N = 100k$ for the ‘table’

Algorithm 1: The Dip'n'Sub algorithm

Input: data set X , significance α , threshold T **Output:** labels

```
1  $k = 1$ ;  $labels = [0, \dots, 0]$ ;  $X_{fin} = []$ 
2 while True do
3    $s = 1$ ;  $\rho = \vec{0}$ 
4    $Q = \log(d)$  features with lowest weighted
     p-values  $\cup$  first  $\log(d)$  components of PCA
5   for each  $\rho_{tmp} \in Q$  do
6     Update  $\rho_{tmp}$  with SGD using Eq. 3.1
7      $s_{tmp} =$  value of Eq. 3.1 using  $\rho_{tmp}$ 
8     if  $s_{tmp} < s$  then
9        $s = s_{tmp}$ ;  $\rho = \rho_{tmp}$ 
10   $P = \{\text{p-value}(\text{Dip}(\overline{C}_i^\rho), |\overline{C}_i^\rho|) \mid i \in [1, k]\}$ 
11  if  $\frac{\text{sum}\{|C_i| \mid i \in [1, k] \wedge P_i < \alpha\}}{N} \geq T$  then
12    for each cluster  $i$  with  $P_i < \alpha$  do
13       $labels_{new} = \text{TailoredDip}(\overline{C}_i^\rho, \alpha)$ 
14      update  $labels$  using  $labels_{new}$ 
15       $X_{fin} =$  combine  $X_{fin}$  and  $\{\rho^T x \mid x \in X\}$ 
16       $X =$  keep features orthogonal to  $\rho$ 
17  else
18    break
19 return  $labels, X_{fin}$ 
```

method as here the calculation of Dip-p-values is not possible. We can observe, that the calculation of Dip-p-values is fastest with our function, although it should be noted that the speed-up relative to the ‘table’ method is only marginal and could be due to implementation details. The differences concerning the calculation time become of practical value, when the number of Dip-p-values to be calculated gets larger. In Table 2 we can see how the algorithms DipMeans, projected DipMeans and SkinnyDip have decreasing runtime, when our method is used instead of the look-up table or bootstrapping. Information about the data sets are given in the supplement (Sec. 2.2). As expected, our function method does not degrade the clustering performance. Across all three algorithms and all data sets, the normalised mutual information (NMI) remains stable with an average difference between ‘table’ and ‘function’ of $9.00 \cdot 10^{-3}$ and $1.17 \cdot 10^{-2}$ between ‘function’ and ‘bootstrap’. Runtime is comparable to the ‘table’ method and improves notably compared to ‘bootstrapping’ as we save 50%, 92% and 99% for DipMeans, projected DipMeans and SkinnyDip, respectively.

4.3 Dip'n'Sub Evaluation We evaluate our algorithm Dip'n'Sub and competitors in terms of cluster-

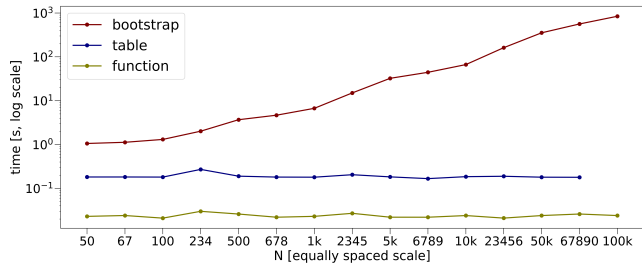


Figure 5: Runtime in seconds [s] on a logarithmic scale for the calculations of 100 Dip-p-values per sample size with the three methods ‘bootstrap’, ‘table’ and ‘function’ summed up over all 23 distribution scenarios as described in the supplement (Sec. 2.3).

ing performance using the normalised mutual information (NMI). This score attains values between 0 and 1, where 0 indicates a purely random label assignment and a value close to 1 is a perfect clustering result.

Comparison Methods: We compare to multiple approaches that define a common subspace for all clusters. This includes dimensionality reduction methods like PCA, ICA or DipExt, which we combine with k-means, and the algorithms LDA-k-means, FOSSCLU and SubKmeans. Furthermore, since Dip'n'Sub is able to estimate the number of clusters, we compare with the Dip-based k -estimation methods DipMeans, projected DipMeans and SkinnyDip.

For PCA, we set the number of components such that 90% of the variance is preserved, and for ICA, it equals k . The significance level is set to 0.01 for all Dip-based methods. The range in which FOSSCLU can determine the number of subspace dimensions with MDL is defined as [1, 5]. All other parameters were set as described in the respective papers. Regarding Dip'n'Sub we set $T = 0.15$ and the significance to 0.01. For SGD, we choose a momentum of 0.95 and a step-size of 0.1 (for USER, ALOI, AIBO, SYMB, OLIVE) or 0.01 (for SYNTH, BANK, HTRU2, MICE, MOTE). Since none of the above data sets contains outliers, we assign all points to the best matching cluster by using the strategy described in Sec. 3.3.

Quantitative Analyses: Table 3 shows the results of our algorithm Dip'n'Sub and our competitors on a wide range of data sets (see supplement Sec. 2.2 for details). Note, that compared to the other subspace algorithms we do not know the ground truth number of clusters. Nevertheless, we are competitive compared to subspace and Dip-based k -estimation methods as we rank first 4 times and second 5 times in terms of NMI. On ALOI, we are slightly inferior, but we only need a single feature for our result. Overall, Dip'n'Sub achieves

Table 1: Dip-p-values for different unimodal (**left**) and multimodal (**right**) distributions with varying sample sizes N . All given values are averages for 100 random samples \pm standard deviation. Respective first, second and third rows per distribution show Dip-p-values calculated with methods ‘table’ (T), ‘function’ (F) and ‘bootstrapping’ (B, 1000 repetitions). Dip-p-values for multimodal distributions are multiplied by 100; *: values obtained by \sqrt{N} -interpolation, †: values not available.

unim. Distr.	Method	$N = 50$	$N = 234$	$N = 2345$	$N = 100k$		multim. Distr.	$N = 50$	$N = 234$	$N = 2345$	$N = 100k$
$\mathcal{N}(4, 1)$	T	0.77 ± 0.24	$0.86 \pm 0.19^*$	$0.97 \pm 0.07^*$	†		$\mathcal{N}(4, 1)$	8.94 ± 15.0	$0.06 \pm 0.23^*$	$0.00 \pm 0.00^*$	†
	F	0.77 ± 0.24	0.86 ± 0.19	0.97 ± 0.07	1.00 ± 0.02		\cup	8.83 ± 14.9	0.09 ± 0.25	0.00 ± 0.00	0.00 ± 0.00
	B	0.77 ± 0.24	0.86 ± 0.19	0.97 ± 0.07	1.00 ± 0.02		$\mathcal{N}(0, 1)$	8.78 ± 15.0	0.06 ± 0.21	0.00 ± 0.00	0.00 ± 0.00
$\mathcal{T}_{nc}(4, 2, 0, 1)$	T	0.80 ± 0.21	$0.89 \pm 0.14^*$	$0.98 \pm 0.03^*$	†		$\mathcal{T}_{nc}(4, 2, 0, 1)$	0.79 ± 2.20	$0.00 \pm 0.00^*$	$0.00 \pm 0.00^*$	†
	F	0.80 ± 0.21	0.90 ± 0.14	0.98 ± 0.03	1.00 ± 0.00		\cup	0.83 ± 2.07	0.00 ± 0.00	0.00 ± 0.00	0.00 ± 0.00
	B	0.80 ± 0.21	0.90 ± 0.14	0.99 ± 0.03	1.00 ± 0.00		$\mathcal{T}_{nc}(4, 2, 7, 1)$	0.74 ± 2.17	0.00 ± 0.00	0.00 ± 0.00	0.00 ± 0.00
$\mathcal{L}(0, 2)$	T	0.85 ± 0.19	$0.95 \pm 0.11^*$	$0.99 \pm 0.04^*$	†		$\mathcal{L}(0, 2)$	24.1 ± 24.9	$2.36 \pm 7.87^*$	$0.00 \pm 0.00^*$	†
	F	0.85 ± 0.19	0.95 ± 0.11	0.99 ± 0.04	1.00 ± 0.00		\cup	23.9 ± 25.1	2.37 ± 7.82	0.00 ± 0.00	0.00 ± 0.00
	B	0.85 ± 0.19	0.95 ± 0.11	0.99 ± 0.04	1.00 ± 0.00		$\mathcal{L}(7, 2)$	23.8 ± 24.8	2.34 ± 8.06	0.00 ± 0.00	0.00 ± 0.00

Table 2: Average NMI and runtime (RT - in seconds) results for DipMeans, p. DipMeans and SkinnyDip using the Dip-p-value calculation methods ‘table’ (T), ‘function’ (F) and ‘bootstrap’ (B) after 10 runs.

Dataset	DipMeans						p. DipMeans						SkinnyDip					
	NMI			RT			NMI			RT			NMI			RT		
	T	F	B	T	F	B	T	F	B	T	F	B	T	F	B	T	F	B
SYNTH	0.64	0.64	0.64	6.87	5.82	8.92	0.86	0.86	0.85	0.76	0.74	9.03	0.16	0.16	0.16	0.02	0.01	14.66
BANK	0.31	0.31	0.30	13.00	6.93	43.71	0.30	0.31	0.30	7.70	5.46	69.81	0.13	0.13	0.13	0.01	0.00	2.56
USER	0.00	0.00	0.00	0.05	0.02	0.08	0.34	0.34	0.35	1.54	1.13	11.37	0.15	0.15	0.15	0.00	0.00	0.68
HTRU2	0.00	0.00	0.00	28.87	28.32	29.03	0.17	0.17	0.17	2.20	2.18	19.05	0.08	0.08	0.08	0.04	0.04	40.78
ALOI	0.96	0.96	0.92	0.43	0.22	0.84	0.49	0.51	0.49	9.03	6.68	54.36	0.17	0.15	0.17	0.06	0.04	3.68
MICE	0.00	0.00	0.00	0.19	0.12	0.27	0.53	0.54	0.53	91.47	50.21	607.21	0.00	0.00	0.00	0.01	0.01	3.76
AIBO	0.00	0.00	0.00	0.09	0.04	0.14	0.28	0.33	0.27	20.02	5.33	129.60	0.02	0.02	0.02	0.02	0.01	3.29
MOTE	0.35	0.35	0.35	0.85	0.62	1.21	0.00	0.00	0.00	0.03	0.02	0.37	0.00	0.00	0.00	0.03	0.02	8.73
SYMB	0.82	0.82	0.82	1.50	1.15	2.23	0.70	0.74	0.70	36.70	5.64	73.69	0.02	0.02	0.02	0.11	0.10	5.16
OLIVE	0.50	0.50	0.50	0.06	0.04	0.16	0.64	0.52	0.64	1.26	0.15	3.08	0.04	0.04	0.04	0.03	0.02	0.39

a good ratio of NMI to the identified number of cluster-relevant features. Our method identifies rather small subspaces (maximum number of features is 3 for BANK, MICE and SYMB), which in combination with the good NMI values suggests that those features are particularly relevant for clustering. This can be interesting for a visual evaluation of the results especially in the unsupervised domain. Furthermore, our estimation of k is notably better than that of other Dip-based methods (which we outperform every time with regard to NMI except for OLIVE). While those procedures identify the correct number of clusters only once, we manage it in 50% of the cases. Especially projected DipMeans seems to heavily overestimate the number of clusters. This confirms our hypothesis that in many cases one can detect additional multimodal structures when looking at a single cluster. Therefore, we benefit from considering only those projection axes relevant to all clusters.

5 Conclusion

In this paper, we propose a differentiable function to translate Dip-values to Dip-p-values. This provides an

automatic and fast translation for any desired sample size. We show that our method is effective as our Dip-p-values show lower squared errors than previously used look-up tables. Further, it is efficient regarding computing time. Finally, we underpin its practical relevance by integrating our function in the subspace clustering algorithm Dip’n’Sub. Here, we show how our proposal enables the use of gradient descent for the Dip-test’s p -value. Future efforts may attempt to integrate those ideas into deep learning applications.

References

- [1] C. C. AGGARWAL AND P. S. YU, *Finding generalized projected clusters in high dimensional spaces*, SIGMOD, ACM, 2000, p. 70–81.
- [2] C. BÖHM, K. KAILING, P. KRÖGER, AND A. ZIMEK, *Computing clusters of correlation connected objects*, SIGMOD, ACM, 2004, p. 455–466.
- [3] L. CAO, P.-J. SHI, L. LI, AND G. CHEN, *A new flexible sigmoidal growth model*, Symmetry, 11 (2019), p. 204.
- [4] T. CHAMALIS AND A. LIKAS, *The projected dip-means clustering algorithm*, SETN, ACM, 2018.

Table 3: Maximum NMI results of different common subspace and Dip-based k -estimation algorithms after 10 runs. The resulting number of clusters and dimensions is given in brackets. Best result in bold, runner-up dotted. (k = number of clusters, d = data set dimensionality, KM = k-means, †: no results due to non-trivial errors).

Dataset (k/d)	Common Subspace Algorithms							Dip-based k -estimation Algorithms		
	Dip'n'Sub	PCA+KM	ICA+KM	DipExt+KM	LDA-KM	SubKM	FOSSCLU	DipMeans	p. DipMeans	SkinnyDip
SYNTH (7/8)	0.97 (7/2)	0.87 (7/4)	0.38 (7/7)	0.69 (7/1)	0.88 (7/6)	0.87 (7/6)	0.90 (7/5)	0.64 (3/8)	0.92 (6/8)	0.16 (2/8)
BANK (2/4)	0.41 (7/3)	0.03 (2/2)	0.01 (2/2)	0.83 (2/1)	0.01 (2/1)	0.03 (2/1)	0.01 (2/4)	0.32 (41/4)	0.32 (36/4)	0.13 (2/4)
USER (4/5)	0.52 (10/1)	0.43 (4/5)	0.03 (4/4)	0.40 (4/2)	0.49 (4/3)	0.46 (4/3)	0.65 (4/2)	0.00 (1/5)	0.36 (33/5)	0.15 (2/5)
HTRU2 (2/8)	0.38 (3/2)	0.03 (2/2)	0.30 (2/2)	0.03 (2/1)	0.28 (2/1)	0.03 (2/1)	0.32 (2/5)	0.00 (1/66)	0.18 (7/66)	0.08 (1/66)
ALOI (4/66)	0.98 (4/1)	1.00 (4/35)	1.00 (4/4)	1.00 (4/5)	1.00 (4/3)	1.00 (4/3)	†	0.96 (5/66)	0.52 (69/66)	0.17 (16/66)
MICE (8/68)	0.55 (6/3)	0.27 (8/6)	0.39 (8/8)	0.59 (8/3)	†	0.29 (8/7)	0.33 (8/5)	0.00 (1/68)	0.54 (278/68)	0.00 (1/68)
AIBO (2/70)	0.68 (2/1)	0.68 (2/20)	0.56 (2/2)	0.60 (2/3)	0.30 (2/1)	0.68 (2/1)	0.52 (2/5)	0.00 (1/70)	0.34 (35/70)	0.02 (3/70)
MOTE (2/84)	0.37 (2/1)	0.30 (2/42)	0.37 (2/2)	0.41 (2/2)	0.28 (2/1)	0.35 (2/1)	0.08 (2/5)	0.36 (3/84)	0.00 (1/84)	0.00 (1/84)
SYMB (6/398)	0.84 (5/3)	0.80 (6/6)	0.79 (6/6)	0.65 (6/2)	0.80 (6/5)	0.80 (6/5)	†	0.82 (5/398)	0.74 (16/398)	0.02 (2/398)
OLIVE (4/570)	0.57 (4/2)	0.68 (4/4)	0.69 (4/4)	0.73 (4/58)	†	0.75 (4/3)	0.16 (4/3)	0.50 (2/570)	0.68 (9/570)	0.04 (1/570)

[5] P. CHASANI AND A. LIKAS, *The wu -test for statistical modeling of unimodal data*, Pattern Recognition, 122 (2022), p. 108272.

[6] Y. CHENG, *Mean shift, mode seeking, and clustering*, IEEE transactions on pattern analysis and machine intelligence, 17 (1995), pp. 790–799.

[7] P. CHRONIS, S. ATHANASIOU, AND S. SKIADOPOULOS, *Automatic clustering by detecting significant density dips in multiple dimensions*, in ICDM, IEEE, 2019, pp. 91–100.

[8] C. H. Q. DING AND T. LI, *Adaptive dimension reduction using discriminant analysis and K-means clustering*, in ICML, vol. 227, ACM, 2007, pp. 521–528.

[9] R. A. FISHER, *The statistical utilization of multiple measurements*, Annals of Eugenics, 8 (1938), pp. 376–386.

[10] S. GOEBL, X. HE, C. PLANT, AND C. BÖHM, *Finding the optimal subspace for clustering*, in ICDM, IEEE, 2014, pp. 130–139.

[11] J. A. HARTIGAN AND P. M. HARTIGAN, *The dip test of unimodality*, Ann. Statist., 13 (1985), pp. 70–84.

[12] A. HYVÄRINEN AND E. OJA, *Independent component analysis: algorithms and applications*, Neural Networks, 13 (2000), pp. 411–430.

[13] A. KALOGERATOS AND A. LIKAS, *Dip-means: an incremental clustering method for estimating the number of clusters*, in Advances in Neural Information Processing Systems, vol. 25, Curran Associates, Inc., 2012.

[14] A. KRAUSE AND V. LIEBSCHER, *Multimodal projection pursuit using the dip statistic*, (2005).

[15] C. LEIBER, L. G. M. BAUER, M. NEUMAYR, C. PLANT, AND C. BÖHM, *The dipencoder: Enforcing multimodality in autoencoders*, in SIGKDD, ACM, 2022, p. 846–856.

[16] C. LEIBER, L. G. M. BAUER, B. SCHELLING, C. BÖHM, AND C. PLANT, *Dip-based deep embedded clustering with k -estimation*, SIGKDD, ACM, 2021, p. 903–913.

[17] Y. LUO, Y. ZHANG, X. DING, X. CAI, C. SONG, AND X. YUAN, *Strdip: A fast data stream clustering algorithm using the dip test of unimodality*, in WISE, Springer, 2018, pp. 193–208.

[18] S. MAURUS AND C. PLANT, *Skinny-dip: Clustering in a sea of noise*, SIGKDD, ACM, 2016, p. 1055–1064.

[19] D. MAUTZ, W. YE, C. PLANT, AND C. BÖHM, *Towards an optimal subspace for k -means*, SIGKDD, ACM, 2017, p. 365–373.

[20] D. MAUTZ, W. YE, C. PLANT, AND C. BÖHM, *Non-redundant subspace clusterings with nr -kmeans and nr -dipmeans*, ACM Trans. Knowl. Discov. Data, 14 (2020), pp. 55:1–55:24.

[21] K. PEARSON, *Liii. on lines and planes of closest fit to systems of points in space*, The London, Edinburgh, and Dublin Philosophical Magazine and Journal of Science, 2 (1901), pp. 559–572.

[22] F. J. RICHARDS, *A Flexible Growth Function for Empirical Use*, Journal of Experimental Botany, 10 (1959), pp. 290–301.

[23] J. H. RICKETTS AND G. A. HEAD, *A five-parameter logistic equation for investigating asymmetry of curvature in baroreflex studies.*, American journal of physiology. Regulatory, integrative and comparative physiology, 277 2 (1999), pp. R441–R454.

[24] B. SCHELLING, L. G. M. BAUER, S. BEHZADI, AND C. PLANT, *Utilizing structure-rich features to improve clustering*, in ECML PKDD, Springer, 2020, pp. 91–107.

[25] B. SCHELLING AND C. PLANT, *Diptransformation: Enhancing the structure of a dataset and thereby improving clustering*, in ICDM, IEEE, 2018, pp. 407–416.

[26] A. SIFFER, P.-A. FOUQUE, A. TERMIER, AND C. LARGOUËT, *Are your data gathered?*, SIGKDD, ACM, 2018, p. 2210–2218.

[27] B. W. SILVERMAN, *Using kernel density estimates to investigate multimodality*, Journal of the Royal Statistical Society: Series B, 43 (1981), pp. 97–99.

[28] A. VEDALDI AND S. SOATTO, *Quick shift and kernel methods for mode seeking*, in European conference on computer vision, Springer, 2008, pp. 705–718.

Supplement to ‘Extension of the Dip-test Repertoire - Efficient and Differentiable p-value Calculation for Clustering’

Lena G. M. Bauer^{*,†,‡} Collin Leiber^{*,§} Christian Böhm[†] Claudia Plant[†]

1 TailoredDip

In the following we explain TailoredDip, which adds two extensions to the UniDip [7] algorithm. First, we show how a cluster can be expanded to include the tails of a distribution and then how outliers can be assigned to an appropriate cluster.

1.1 Capturing the Tails As mentioned in the paper, UniDip has problems correctly identifying the tails of distributions. These are usually labeled as noise. This behavior can be observed in Fig. 1a. The Gaussian clusters are not completely captured, but only the densest parts of the distributions. The same applies when uniformly distributed noise is added to the data (see Fig. 1c). TailoredDip is superior in capturing the tails of the distributions in both cases. This is also confirmed by the normalised mutual information (NMI) score and can be seen in Fig. 1b and 1d. We achieve this improvement by checking the spaces between the clusters for additional structures after the regular UniDip algorithm has terminated. Although these structures are no longer significant enough to be regarded as independent clusters by UniDip, they can still be part of a cluster. Therefore, we mirror the respective area between two clusters and calculate the Dip-p-value. If this indicates that there are still multimodal structures left, we again search for appropriate modes. In order to check whether a found structure matches the adjacent clusters, we apply a strategy that has been described in [6]. Here, the closest $2|S|$ samples of the respective cluster combined with the newly found structure S are used to calculate the Dip-p-value. If this value indicates unimodality, the structure will be added to that cluster and the process is repeated. The described procedure is shown in Algorithm 1. Since in our case a lot of Dip-p-values have to be calculated, a fast calculation of Dip-p-values is favourable.

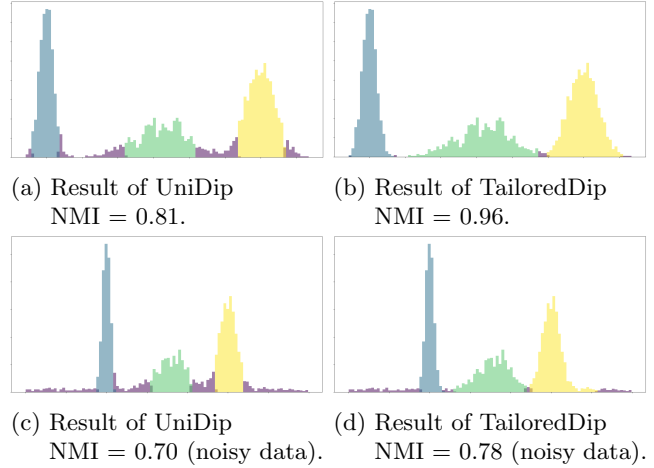


Figure 1: Results of TailoredDip and UniDip on a sample data set consisting of three Gaussian clusters. The identified clusters are coloured in blue, green, and yellow respectively. Outliers are shown in purple.

1.2 Assigning Noise We also present a strategy for assigning outliers to clusters, paying attention to the different tails of the surrounding distributions. In terms of one-dimensional data, it makes sense to define a threshold between every two clusters, indicating whether an outlier is more likely to belong to the left or right cluster. A naive approach would now be to simply set the midpoint between the end of the left and the start of the right cluster. This strategy was chosen in [5], for example. However, this approach completely ignores the existing structures, since it is irrelevant whether a cluster ends abruptly (e.g. in case of a uniform distribution) or fades out slowly (e.g. in case of a normal distribution). To pay attention to these properties, we consider the Empirical Cumulative Distribution Function (ECDF), which is also used to calculate the Dip-value. Here, we draw a straight line from the last point of the left cluster to the first point of the right cluster. In Fig. 2 this is represented by the dotted red line. We now define the intersection of this line with the ECDF of the data as the cluster boundary. Looking at this point in Fig. 2 (left vertical line) we can see that it separates

^{*}Authors contributed equally.

[†]Faculty of Computer Science, ds:UniVie, University of Vienna, Vienna, Austria. {lena.bauer, christian.boehm, claudia.plant}@univie.ac.at

[‡]UniVie Doctoral School Computer Science.

[§]LMU Munich & MCML, Munich, Germany. leiber@dbs.ifi.lmu.de

Algorithm 1: The TailoredDip algorithm

Input: one-dimensional data set X ,
significance α

Output: labels

```
1 // Get initial clusters by running UniDip
2 labels, k = UniDip(X,  $\alpha$ )
3 for  $i = 0; i \leq k; i += 1$  do
4   if  $i == 0$  then
5     |  $X_{\text{sub}} =$  samples left of first cluster
6   else if  $i == k$  then
7     |  $X_{\text{sub}} =$  samples right of last cluster
8   else
9     |  $X_{\text{sub}} =$  samples between cluster  $i$  and
     |  $i + 1$ 
10 // Is  $X_{\text{sub}}$  uniformly distributed (only
    noise)?
11  $X_{\text{mirror}} =$  mirror  $X_{\text{sub}}$ 
12  $p =$  p-value(Dip( $X_{\text{mirror}}$ ),  $|X_{\text{mirror}}|$ )
13 if  $p < \alpha$  then
14   | labelsnew,  $k_{\text{new}} =$  UniDip( $X_{\text{sub}}$ ,  $\alpha$ )
15   |  $X_{\text{first}} =$  combine cluster  $i$  with the first
     | new cluster // (ignore if  $i == 0$ )
16   |  $p_{\text{first}} =$  p-value(Dip( $X_{\text{first}}$ ),  $|X_{\text{first}}|$ )
17   |  $X_{\text{last}} =$  combine cluster  $i + 1$  with the
     | last new cluster // (ignore if  $i == k$ )
18   |  $p_{\text{last}} =$  p-value(Dip( $X_{\text{last}}$ ),  $|X_{\text{last}}|$ )
19   | if  $i \neq 0$  and  $p_{\text{first}} \geq \alpha$  and ( $k_{\text{new}} \neq 1$  or
     |  $p_{\text{first}} \geq p_{\text{last}}$ ) then
20   | | Update labels by adding all entries
     | | with labelsnew == 1 to cluster  $i$ 
21   | else if  $i \neq k$  and  $p_{\text{last}} \geq \alpha$  and
     | ( $k_{\text{new}} \neq 1$  or  $p_{\text{last}} > p_{\text{first}}$ ) then
22   | | Update labels by adding all entries
     | | with labelsnew ==  $k_{\text{new}}$  to cluster
     | |  $i + 1$ 
23   | if Cluster  $i$  or  $i + 1$  was updated then
24   | | go to line 4
25 return labels
```

the tails of the two distributions much better than the naive strategy (right vertical line) since it better captures the higher standard deviation of the right cluster. If more than one intersection occurs, we choose the one closest to the midpoint between the clusters.

2 Additional Information for the Experiments

2.1 Computational Setup Dip'n'Sub as well as the algorithms DipMeans [4], projected DipMeans [1], SkinnyDip [7], DipExt [9], LDA-k-means [2] and SubKmeans [8] are all implemented in Python. Regarding FOSS-

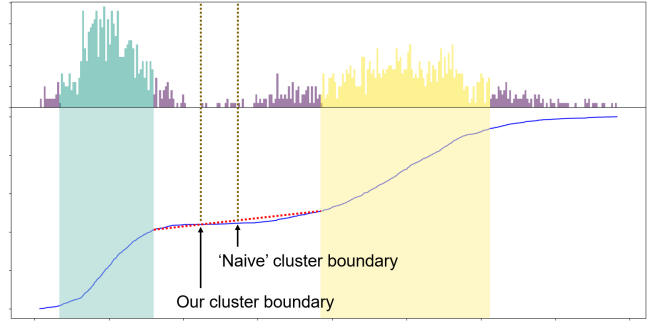


Figure 2: Visualisation of our strategy to assign outliers to the neighbouring clusters. [Top] A histogram of the data. The left (teal) cluster originates from a $\mathcal{N}(0, 1)$ distribution with 700 samples, the right (yellow) cluster originates from a $\mathcal{N}(10, 2.5)$ distribution with 900 samples. The outliers are shown in purple. [Bottom] The ECDF of the data is shown in blue. The areas of the clusters are highlighted in their respective colours. The dotted red line indicates the connection line between the end of the teal and the beginning of the yellow cluster. The right vertical brown line marks the position of a naive cluster boundary, which corresponds to the centre of the red line. Our boundary corresponds to the intersection of the red line with the ECDF and captures the different tails of the two clusters much better.

CLU [3] we use the Java implementation as referenced in the paper. We conduct all runtime experiments on a machine with an Intel Core i7-5600U CPU with 2.60GHz and 8GB RAM. Further, we use Python 3.7 and in case of FOSSCLU, we use Java 8 due to compatibility issues.

2.2 Data Sets We conduct experiments on 9 real world data sets and one synthetic data set (the latter can be seen in the main paper in Fig. 4). Banknotes (BANK), User Knowledge (USER), HTRU2 and Mice Protein (MICE) are numerical data sets from the UCI repository¹. SonyAIBO (AIBO), MoteStrain (MOTE), Symbols (SYMB) and OliveOil (OLIVE) are time series data sets², and ALOI³ is an image data collection. ALOI was preprocessed as described in [10], resulting in 288 samples divided into 4 clusters. Other than ALOI, no data set did receive any pre-processing, except that features with a variance of 0 were removed. Note, that TailoredDip only works with continuous features, otherwise each value can be recognized as a separate mode. A summary of the data sets is given in Table 1.

¹<https://archive.ics.uci.edu>

²<https://www.timeseriesclassification.com>

³<https://aloi.science.uva.nl/>

Table 1: Summary of the data sets (N = number of data points, d = dimensionality, k = number of clusters).

Dataset	N	d	k
SYNTH	6,300	8	7
BANK	1,372	4	2
USER	403	5	4
HTRU2	17,898	8	2
ALOI	288	66	4
MICE	1,077	68	8
AIBO	621	70	2
MOTE	1,272	84	2
SYMB	1,020	398	6
OLIVE	60	570	4

2.3 Interpolate Look-up Table We would like to briefly explain how missing values in the state-of-the-art look-up table are interpolated. Basically two interpolations must be performed. First, the values for the number of samples that lie below and above the input N must be searched for in the table. By using these two values we are able to interpolate all relevant (Dip, p)-pairs in relation to \sqrt{N} . In this interpolated array we search for the Dip-values that are below and above our input Dip to interpolate the Dip-p-value linearly.

2.4 Large Distribution Table In Tables 2 and 3 we show Dip-p-value calculations with the three methods ‘table’ (T), ‘function’ (F) and ‘bootstrap’ (B) for samples of 15 different sample sizes and a total of 23 distribution scenarios. In all cases, we can observe that our fitted function produces basically the same Dip-p-values as the other two methods. For this evaluation we first consider 8 different unimodal distributions:

- $\mathcal{N}(a, b)$... normal distribution with mean a and standard deviation b
- $\mathcal{T}(d, a, b)$... students-t distribution with d degrees of freedom, centre a and scaling b
- $\mathcal{L}(a, b)$... Laplace distribution with centre a and scaling b
- $\mathcal{U}(a, b)$... uniform distribution between a and b
- $\mathcal{G}(s, a, b)$... Gamma distribution with shape parameter s , centre a and scaling b
- $\mathcal{E}(a, b)$... exponential distribution with centre a and scaling b
- $\mathcal{B}(s, r, a, b)$... Beta distribution with shape parameters s and r , centre a and scaling b

- $\mathcal{T}_{nc}(d, c, a, b)$... non central students-t distribution with d degrees of freedom, non centrality c , centre a and scaling b

First, Table 2 shows results for these distributions, with only the listed distributions involved individually. We then generate 8 multimodal distributions by combining $\frac{N}{2}$ samples from one distribution with $\frac{N}{2}$ samples from the same distribution with a different centre. Additionally, we consider 7 cases, where we generate samples by choosing half the points from $\mathcal{N}(4, 1)$ and the other half from one of the other unimodal distributions. These combinations always show multimodal structure. An exception is the case of samples from $\mathcal{N}(4, 1) \cup \mathcal{T}_{nc}(4, 2, 0, 1)$. We include this combination to have a relatively unambiguous case between unimodal and multimodal. Our function performs reliably in all cases as can be seen in Table 3.

References

- [1] T. CHAMALIS AND A. LIKAS, *The projected dip-means clustering algorithm*, SETN, ACM, 2018.
- [2] C. H. Q. DING AND T. LI, *Adaptive dimension reduction using discriminant analysis and K-means clustering*, in ICML, vol. 227, ACM, 2007, pp. 521–528.
- [3] S. GOEBL, X. HE, C. PLANT, AND C. BÖHM, *Finding the optimal subspace for clustering*, in ICDM, IEEE, 2014, pp. 130–139.
- [4] A. KALOGERATOS AND A. LIKAS, *Dip-means: an incremental clustering method for estimating the number of clusters*, in Advances in Neural Information Processing Systems, vol. 25, Curran Associates, Inc., 2012.
- [5] C. LEIBER, L. G. M. BAUER, M. NEUMAYR, C. PLANT, AND C. BÖHM, *The dipencoder: Enforcing multimodality in autoencoders*, in SIGKDD, ACM, 2022, p. 846–856.
- [6] C. LEIBER, L. G. M. BAUER, B. SCHELLING, C. BÖHM, AND C. PLANT, *Dip-based deep embedded clustering with k-estimation*, SIGKDD, ACM, 2021, p. 903–913.
- [7] S. MAURUS AND C. PLANT, *Skinny-dip: Clustering in a sea of noise*, SIGKDD, ACM, 2016, p. 1055–1064.
- [8] D. MAUTZ, W. YE, C. PLANT, AND C. BÖHM, *Towards an optimal subspace for k-means*, SIGKDD, ACM, 2017, p. 365–373.
- [9] B. SCHELLING, L. G. M. BAUER, S. BEHZADI, AND C. PLANT, *Utilizing structure-rich features to improve clustering*, in ECML PKDD, Springer, 2020, pp. 91–107.
- [10] W. YE, S. MAURUS, N. HUBIG, AND C. PLANT, *Generalized independent subspace clustering*, in ICDM, IEEE, 2016, pp. 569–578.

Table 2: Dip-p-values for different unimodal distributions with varying sample sizes N . All given values are averages for 100 random samples \pm standard deviation. Respective first, second and third rows per distribution show Dip-p-values calculated with methods ‘table’ (T), ‘function’ (F) and ‘bootstrapping’ (B, 1000 repetitions); *: values obtained by \sqrt{N} -interpolation, †: values not available.

Distr.	Meth.	$N = 50$	$N = 67$	$N = 100$	$N = 234$	$N = 500$	$N = 678$	$N = 1k$	$N = 2345$	$N = 5k$	$N = 6789$	$N = 10k$	$N = 23456$	$N = 50k$	$N = 67890$	$N = 100k$	
$\mathcal{N}(4,1)$	T	0.77 ± 0.24	0.81 ± 0.21*	0.80 ± 0.20	0.86 ± 0.19*	0.91 ± 0.14	0.94 ± 0.13*	0.94 ± 0.09	0.97 ± 0.07*	0.99 ± 0.03	0.98 ± 0.05*	0.99 ± 0.04	0.99 ± 0.01*	1.00 ± 0.02	1.00 ± 0.01*	1.00 ± 0.01	†
	F	0.77 ± 0.24	0.81 ± 0.21	0.81 ± 0.20	0.86 ± 0.19	0.91 ± 0.14	0.94 ± 0.13	0.95 ± 0.09	0.97 ± 0.07	0.99 ± 0.03	0.98 ± 0.05	0.99 ± 0.04	1.00 ± 0.01	1.00 ± 0.02	1.00 ± 0.01	1.00 ± 0.01	1.00 ± 0.02
	B	0.77 ± 0.24	0.81 ± 0.21	0.81 ± 0.20	0.86 ± 0.19	0.91 ± 0.14	0.94 ± 0.13	0.95 ± 0.09	0.97 ± 0.07	0.99 ± 0.03	0.98 ± 0.05	0.99 ± 0.04	1.00 ± 0.01	1.00 ± 0.02	1.00 ± 0.01	1.00 ± 0.01	1.00 ± 0.02
$\mathcal{T}(4,0,1)$	T	0.78 ± 0.22	0.85 ± 0.19*	0.84 ± 0.20	0.88 ± 0.18*	0.94 ± 0.10	0.95 ± 0.09*	0.97 ± 0.07	0.97 ± 0.07*	0.99 ± 0.04	0.99 ± 0.04	0.99 ± 0.03*	0.99 ± 0.02	1.00 ± 0.01*	1.00 ± 0.00	1.00 ± 0.01*	†
	F	0.78 ± 0.22	0.85 ± 0.19	0.85 ± 0.20	0.88 ± 0.18	0.94 ± 0.10	0.96 ± 0.09	0.97 ± 0.07	0.97 ± 0.07	0.99 ± 0.04	0.99 ± 0.04	0.99 ± 0.03	0.99 ± 0.02	1.00 ± 0.01	1.00 ± 0.00	1.00 ± 0.01	1.00 ± 0.00
	B	0.78 ± 0.22	0.85 ± 0.19	0.85 ± 0.20	0.88 ± 0.18	0.94 ± 0.10	0.96 ± 0.09	0.97 ± 0.07	0.97 ± 0.07	0.99 ± 0.04	0.99 ± 0.04	0.99 ± 0.03	0.99 ± 0.02	1.00 ± 0.01	1.00 ± 0.00	1.00 ± 0.01	1.00 ± 0.00
$\mathcal{L}(0,2)$	T	0.85 ± 0.19	0.88 ± 0.18*	0.92 ± 0.11	0.95 ± 0.11*	0.98 ± 0.04	0.98 ± 0.04*	0.99 ± 0.01	0.99 ± 0.04*	1.00 ± 0.00	1.00 ± 0.00	1.00 ± 0.00*	1.00 ± 0.00*	1.00 ± 0.00*	1.00 ± 0.00*	1.00 ± 0.00*	†
	F	0.85 ± 0.19	0.89 ± 0.18	0.92 ± 0.11	0.95 ± 0.11	0.98 ± 0.04	0.99 ± 0.04	0.99 ± 0.01	0.99 ± 0.04	1.00 ± 0.00	1.00 ± 0.00	1.00 ± 0.00	1.00 ± 0.00	1.00 ± 0.00	1.00 ± 0.00	1.00 ± 0.00	1.00 ± 0.00
	B	0.85 ± 0.19	0.89 ± 0.18	0.92 ± 0.11	0.95 ± 0.11	0.98 ± 0.04	0.99 ± 0.03	1.00 ± 0.01	0.99 ± 0.04	1.00 ± 0.00	1.00 ± 0.00	1.00 ± 0.00	1.00 ± 0.00	1.00 ± 0.00	1.00 ± 0.00	1.00 ± 0.00	1.00 ± 0.00
$\mathcal{I}(0,2)$	T	0.52 ± 0.29	0.50 ± 0.28*	0.46 ± 0.28	0.53 ± 0.29*	0.52 ± 0.28	0.54 ± 0.31*	0.48 ± 0.30	0.50 ± 0.28*	0.56 ± 0.28	0.56 ± 0.28	0.54 ± 0.29*	0.52 ± 0.32	0.50 ± 0.30*	0.53 ± 0.28	0.51 ± 0.30*	†
	F	0.52 ± 0.30	0.51 ± 0.28	0.46 ± 0.28	0.53 ± 0.30	0.52 ± 0.29	0.54 ± 0.31	0.48 ± 0.30	0.49 ± 0.29	0.56 ± 0.28	0.56 ± 0.28	0.54 ± 0.30	0.52 ± 0.32	0.50 ± 0.30	0.53 ± 0.28	0.51 ± 0.30	0.56 ± 0.28
	B	0.52 ± 0.29	0.51 ± 0.28	0.46 ± 0.28	0.53 ± 0.30	0.52 ± 0.29	0.54 ± 0.31	0.48 ± 0.30	0.50 ± 0.29	0.56 ± 0.28	0.56 ± 0.28	0.54 ± 0.30	0.52 ± 0.32	0.50 ± 0.30	0.53 ± 0.28	0.51 ± 0.31	0.56 ± 0.28
$\mathcal{G}(2,-1,1)$	T	0.76 ± 0.24	0.79 ± 0.22*	0.79 ± 0.22	0.88 ± 0.14*	0.91 ± 0.14	0.91 ± 0.11*	0.93 ± 0.13	0.97 ± 0.08*	0.99 ± 0.05	0.99 ± 0.05	0.99 ± 0.05	0.99 ± 0.02	1.00 ± 0.01*	1.00 ± 0.01	1.00 ± 0.00*	†
	F	0.76 ± 0.24	0.79 ± 0.22	0.81 ± 0.21	0.88 ± 0.14	0.91 ± 0.14	0.92 ± 0.11	0.94 ± 0.13	0.97 ± 0.08	0.99 ± 0.05	0.99 ± 0.05	0.99 ± 0.05	0.99 ± 0.02	1.00 ± 0.02	1.00 ± 0.01	1.00 ± 0.00	1.00 ± 0.00
	B	0.76 ± 0.23	0.79 ± 0.22	0.81 ± 0.21	0.88 ± 0.14	0.91 ± 0.14	0.92 ± 0.11	0.94 ± 0.13	0.98 ± 0.08	0.99 ± 0.05	0.99 ± 0.05	0.99 ± 0.05	0.99 ± 0.02	1.00 ± 0.01	1.00 ± 0.00	1.00 ± 0.00	1.00 ± 0.00
$\mathcal{E}(0,1)$	T	0.72 ± 0.26	0.79 ± 0.21*	0.79 ± 0.23	0.86 ± 0.18*	0.92 ± 0.11	0.95 ± 0.10*	0.94 ± 0.11	0.98 ± 0.05*	0.99 ± 0.03	0.99 ± 0.03	0.99 ± 0.02*	1.00 ± 0.01	1.00 ± 0.00*	1.00 ± 0.00	1.00 ± 0.00*	†
	F	0.72 ± 0.26	0.79 ± 0.21	0.80 ± 0.23	0.86 ± 0.18	0.93 ± 0.11	0.95 ± 0.10	0.94 ± 0.11	0.98 ± 0.05	0.99 ± 0.04	1.00 ± 0.02	1.00 ± 0.01	1.00 ± 0.00	1.00 ± 0.00	1.00 ± 0.00	1.00 ± 0.00	1.00 ± 0.00
	B	0.72 ± 0.26	0.79 ± 0.21	0.79 ± 0.23	0.86 ± 0.18	0.93 ± 0.11	0.95 ± 0.10	0.94 ± 0.11	0.98 ± 0.05	0.99 ± 0.04	1.00 ± 0.02	1.00 ± 0.01	1.00 ± 0.00	1.00 ± 0.00	1.00 ± 0.00	1.00 ± 0.00	1.00 ± 0.00
$\mathcal{B}(2,2,1,1)$	T	0.65 ± 0.25	0.66 ± 0.25*	0.73 ± 0.25	0.81 ± 0.18*	0.82 ± 0.22	0.84 ± 0.21*	0.84 ± 0.21	0.90 ± 0.16*	0.96 ± 0.07	0.96 ± 0.07	0.96 ± 0.09*	0.98 ± 0.05*	0.98 ± 0.05*	0.99 ± 0.02	0.99 ± 0.01*	†
	F	0.65 ± 0.25	0.67 ± 0.26	0.73 ± 0.26	0.82 ± 0.18	0.82 ± 0.22	0.84 ± 0.21	0.85 ± 0.21	0.90 ± 0.16	0.96 ± 0.07	0.96 ± 0.07	0.96 ± 0.09	0.98 ± 0.05	0.99 ± 0.05	0.99 ± 0.02	1.00 ± 0.01	0.99 ± 0.02
	B	0.65 ± 0.26	0.66 ± 0.25	0.73 ± 0.25	0.81 ± 0.19	0.82 ± 0.22	0.84 ± 0.21	0.84 ± 0.21	0.90 ± 0.16	0.96 ± 0.07	0.96 ± 0.07	0.97 ± 0.09	0.98 ± 0.05	0.99 ± 0.05	0.99 ± 0.02	1.00 ± 0.01	1.00 ± 0.02
$\mathcal{T}_{nc}(4,2,0,1)$	T	0.80 ± 0.21	0.78 ± 0.23*	0.85 ± 0.17	0.89 ± 0.14*	0.96 ± 0.06	0.94 ± 0.10*	0.95 ± 0.08	0.98 ± 0.03*	0.99 ± 0.04	0.99 ± 0.04	0.99 ± 0.02*	1.00 ± 0.01*	1.00 ± 0.00	1.00 ± 0.00	1.00 ± 0.00*	†
	F	0.80 ± 0.21	0.78 ± 0.23	0.85 ± 0.17	0.90 ± 0.14	0.96 ± 0.06	0.95 ± 0.10	0.96 ± 0.08	0.98 ± 0.03	0.99 ± 0.04	0.99 ± 0.04	0.99 ± 0.02	1.00 ± 0.01	1.00 ± 0.01	1.00 ± 0.00	1.00 ± 0.00	1.00 ± 0.00
	B	0.80 ± 0.21	0.78 ± 0.23	0.85 ± 0.17	0.90 ± 0.14	0.96 ± 0.06	0.95 ± 0.10	0.96 ± 0.08	0.99 ± 0.03	0.99 ± 0.04	0.99 ± 0.04	0.99 ± 0.02	1.00 ± 0.01	1.00 ± 0.01	1.00 ± 0.00	1.00 ± 0.00	1.00 ± 0.00

